Numerical Methods in Civil Engineering, 9-4 (2025) 41-50

Numerical Methods in Civil Engineering

Journal Homepage: https://nmce.kntu.ac.ir/

Evaluation of seismic performance of steel frames with Y-shape braces under far-field and near-field earthquakes

Saeed Najafi*, Shahin Borzoo, Kaveh Saboohian***, Hadi Aboutalebi******

ARTICLE INFO

RESEARCH PAPER

Article history:
Received:
February 2025
Revised:
March 2025
Accepted:
April 2025

Keywords:
Nonlinear dynamic analysis; Y-shape bracing; near-field and far-field Earthquake; Nonlinear dissipated energy, Plastic hinge.

Abstract:

In this study, the finite element modeling of the Y-shape bracing system is initially developed and verified. Next, the seismic performance of steel frames with Y-shape braces under far-field and near-field earthquakes was evaluated. For this purpose, seismic analysis was performed using 12 seismic records including near-field and far-field on 4, 8, and 12-floor structures equipped with and without Y-shape bracing. A series of time history analyses were performed on the samples, which led to the precise review of the Y-shape bracing system. The results show that structures equipped with Y-shape braces have less lateral displacement and also less number and level of plastic hinges; and, the level of non-linear dissipated energy is higher in those structures. Also, the plastic hinges based on the failure indices of the structures indicate that -near-field earthquakes have a more destructive effect of about 20% higher than far earthquakes on structures equipped with Y-shape bracing. Y-shaped bracing has reduced the permanent displacement in the system by up to 30%.

1. Introduction

In earthquake design methods of buildings, three main objectives should be developed: strength, stiffness, and energy absorption capacity. Since the stiffness and ductility of the structure are usually opposite to each other, a reasonable balance between these factors based on economic principles is desirable [1]. In Chevron braced frames, as lateral load increases, the compression bracing tends buckle, leading to a reduction in its axial capacity, while the tensile bracing forces are increased. In this case, at the junction of the brace to the beam, a large unbalanced vertical force is developed, which can cause large deformations in the beam. The adverse effect of this unbalanced vertical force can be eliminated by adding zipper elements between the connection points of the braces to the beams. Zippers connect the lower floor, which is mostly in high demand to the upper floor, which has a safer condition. Therefore, the performance of the structure becomes more uniform, and the demanded ductility in different floors will eventually absorb more energy.

To solve the problem of low stiffness in a flexural frame system and also the effects of low ductility in a frame with concentric bracing, excentric bracing is proposed [2]. Furthermore, one of the considered solutions to solve the problem of openings in bracing systems without any architectural disruption is the Y-shaped bracing system [3].

In recent years, to use more space in the facade of buildings and the possibility of large openings in the presence of this brace many researches have been conducted about the Y-shape bracing system. In new methods of structural design, using appropriate details of energy dissipation methods in the structures, the dimensions of elements that are used in the structure are reduced significantly, which improves the performance of the structure [4], [5]. Although Y-shape braces have high strength and stiffness but their ductility would be affected by buckling and their configuration. The

*PhD Student, Department of Earthquake Engineering, Tarbiat Modares University, Tehran, Iran.

**Corresponding author: Assistant professor, Civil Engineering Department, Technical University of Buein Zahra, Buein Zahra, Qazvin, 3451745346, Iran, Sh.borzoo@bzte.ac.ir

***PhD Student, Department of Civil Engineering, Science and Research Branch, Islamic Azad University, Tehran, Iran.

****PhD Student, Department of Civil Engineering, Shahrkurd Branch, Islamic Azad University, Shahrkurd, Iran.

https://doi.org/10.61186/NMCE.2505.1088

buckling failure is probable in their longest element. One of the best methods to reduce such damages is using dampers in diagonal elements to improve ductility and reduce plastic displacements [6]. Also yielding dampers such as knee joints would improve the seismic behavior of moment frames. Brace elements in this system join to knee joints and after yielding the energy will be dissipated. The Braces would increase stiffness while the knee element produces ductility like a yielding damper [7]. In 2022 Shahiditabar et al., used the methodology recommended by FEMA P695 to evaluate the seismic performance of the self-centered y-shaped (SCY) braced frames. They constructed twenty archetype models and then the collapse of the archetype models evaluated through incremental dynamic analyses (IDA) and pushover analyses. Their research showed that the secondary stiffness and length of the self-centering (SC) element are the key parameters that influence the overall behavior of the SCY-braced frame [8].

In 2022 Mazzolani et al investigated a kind of steel eccentric bracing with vertical shear link (inverted Y-bracing) for seismic retrofitting of an existing building in a high seismic zone. This vertical shear link was evaluated using static nonlinear analysis and had consistency with new seismic regulations. Also, it was efficient in improvement of seismic performance, increasing stiffness and resistance [9].

In 2021 Li et al examined real-time hybrid simulation (RTHS), as an economical, and reliable seismic testing technology for structural analysis. They applied RTHS on the space structure to examine a high-strength steel frame with Y-shaped eccentric braces (HSYE). The proposed RTHS method was utilized in the upper stories of the prototype as the experimental substructure, and the lower stories were taken as the numerical substructure and simulated in finite element software. Then, the OpenFresco test platform and xPC-Target with an adaptive feed-forward delay compensator were used to determine real-time loading. The seismic behavior of the HSYE was tested using selected seismic acceleration records. The results revealed that the RTHS results are stable and reliable. Under an earthquake-simulated loading, the HSYE structure resisted the local energy dissipation characteristics of the shear link and ensured the elasticity of the main frame [10].

In 2025 Minaei et al investigated Incremental Dynamic Analysis (IDA) on two 8- and 12-story BRBF structures under far-fault and near-fault ground motions. Their results suggest the importance of considering near-fault ground motions in assessing BRBF seismic performance, particularly for taller structures [11]. On the other hand, the importance of the pulses of near-fault earthquakes is investigated in the seismic response of mid-rise structures with a triple friction pendulum isolator (TFPI) [12]. These researches show that the near-field records should be considered in the dynamic analysis.

In the present article, at first the finite element modeling of Y-shape bracing system is developed and verified. Subsequently, the behavior of steel structures equipped with the Y-shape braces has been compared and evaluated for near and far-field earthquakes. The effect of braces on the seismic behavior of structures and their ductility has been evaluated. Finally, by measuring the amount of dissipated energy in each of the structures, a logical conclusion has been made regarding the seismic performance of this system.

The novelty of the present study is in the investigation of structures with different elevation levels equipped with Y-shaped bracing under far-field and especially near-field earthquakes. The main basis of comparison in this study is the use of structural parameters, especially energy, to demonstrate the superiority of the aforementioned structural system in dealing with near-field pulses in tall structures.

2. Methodology

The braced frame shown in Figure 1 is idealized as a simple truss. l_1, l_2 and l_3 are the lengths of members 1, 2, and 3, respectively. The initial lengths of the members are assumed as l_{10}, l_{20} and l_{30}. Once the load is applied, the lengths of the braces change as follows [13]:

$$l_i = l_{i0} + \frac{F_i l_{i0}}{EA_i} \quad (1)$$

where l_{io} and l_i are the initial and final lengths of member i. A_i is the cross-sectional area, E is the modulus of elasticity and F_i is the axial force of the member i. By neglecting the axial deformation of the beam and the columns, the new geometry can be determined as follows [13]:

$$\beta = 2tan^{-1}\frac{K_2}{S_2 - l_3} \quad (2)$$

$$\gamma = 2tan^{-1}\frac{K_1}{S_1 - l_2} \quad (3)$$

$$\alpha = 2tan^{-1}\frac{K_1}{S_1 - l_3} \quad (4)$$

$$\gamma_1 = 2tan^{-1}\frac{K_2}{S_2 - l_1} \quad (5)$$

$$\theta = \gamma_1 + \gamma - \pi/2 \quad (6)$$

where

$$S_1 = \frac{l_2 + l_3 + l}{2} \quad (7)$$

$$S_2 = \frac{l_1 + l_3 + h}{2} \quad (8)$$

$$K_1 = \sqrt{\frac{(S_1 - l_3)(S_1 - l_2)(S_1 - l)}{S_1}} \quad (9)$$

$$K_2 = \sqrt{\frac{(S_2 - l_3)(S_2 - l_1)(S_2 - h)}{S_2}} \quad (10)$$

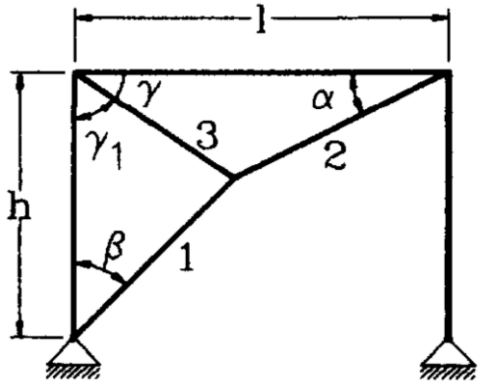

Fig. 1: Y-shape brace idealized as a simple truss [13]

2.1 Numerical modeling

In this research, Abaqus software was used to validate the model. The validation of the Y-shape brace is done based on the Zamani et al research [14]. The model number 1100-5 from Zamani et al (2012) were selected to assess as the validation model and a good correspondence is observed between the results. The cross-sections of structural elements used in the validation model are shown in Table 1. The connections are modeled using the tie constraint in the interaction module to simulate plate welding on the two sides of braces. The material of the flange and web of sections and steel plates were assigned based on their strength and elongation properties in Zamani et al. research [14]. Steel material is in the class of S235 strength grade according to EN10025-2 [15]. Figure 2 shows the details of the connections of the y-braced model. Double plate gussets have been proportioned such that their flexural strength surpasses the connected braces.

The dimensions and the type of mesh element were effective in the precision of outputs. The C3D10 element was used to obtain the results that were almost consistent with the experimental research. To define the strain-stress behavior in the Abaqus, the data related to the tensile test of the steel sample is used. For converting engineering strain-stress to true strain-stress the following equations are used:

$$\varepsilon_{True} = In\left(1 + \varepsilon_{Eng}\right) \quad (11)$$

$$\sigma_{True} = \sigma_{Eng}\left(1 + \varepsilon_{Eng}\right) \quad (12)$$

In the above equations, σ represents the stress and ε represents the strain. In Figure 3, the result of the tensile test for a low-carbon steel sample is presented. The engineering stress and strain values are obtained by experiment.

Table 1: Cross section of rolled structural shapes in validation model [14]

Section	Section height h(mm)	Flange width b (mm)	Flange thickness t (mm)	Web thickness s (mm)	Section area A (mm2)
I180	180	91	8	5.3	2390
U100	100	46	8.5	4.5	1250
IPB200	200	200	15	9	7810

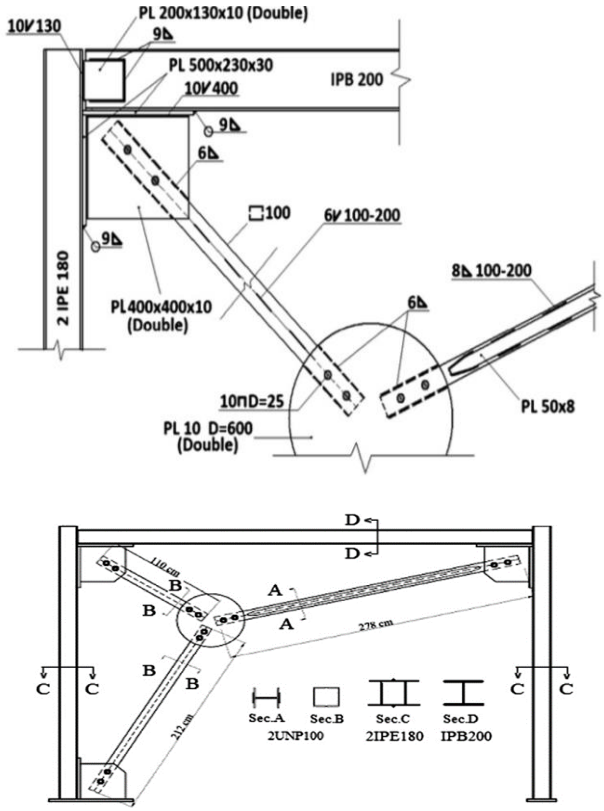

Fig. 2: Details of the validation model [14]

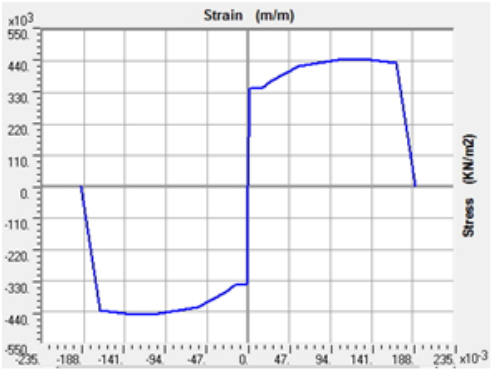

Fig. 3: Stress-Strain curve of ST-37 steel [16]

The boundary conditions and the cyclic loading are applied in the finite element model (Figure 4).

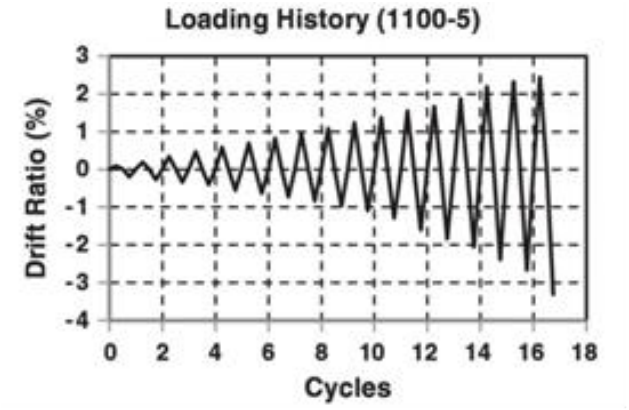

Fig. 4: Applied cyclic loading protocol [14]

Figure 5 shows the final displacement and buckling of the Y-shape brace in the conducted experimental study [14]. Also, as shown in Figure 5, buckling is the same in both experimental and finite elemnt models. Also, Figure 6 shows the hysteresis load-displacement diagram of the finite element model against the exprimental model response.

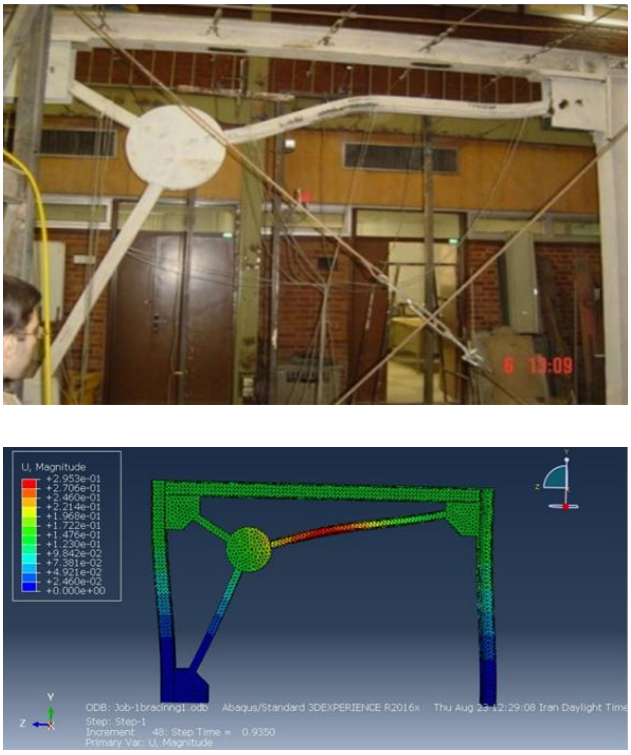

Fig. 5: Final deformation of the Y-shape brace in experimental study and finite element model [14]

2.2 Selecting seismic records

To ensure the seismic performance of Y-shaped braces, their behavior should be measured under the near and far-field earthquakes. The far-field and the near-field records were selected from Gorai et al research in 2019 [17]. In selecting the near-field records three important features such as forward directivity, fling-step, and no-pulse near-field earthquakes are considered. After that, the models are subjected to the nonlinear time history analysis.

To perform dynamic analysis and to compare the results of equivalent nonlinear static analysis with the modeled structures, 6 seismic near-field and 6 far-field records are selected. The selection of these earthquakes was based on the date of their occurrence (recent earthquakes), their strength, the distance from the fault, and the similarity of the soil bed. A summary of information about these earthquakes is given in Table 2.

In near-fault areas, records have a high frequency content. Strong motions of near-field earthquakes, which are characterized by large amplitude, long period, and pulse-like excitations, tend to cause large displacements in the buildings. In this study, it is tried to study the behavior of buildings equipped with Y-shape braces, under the effect of near and far-field earthquakes. In Figure 7, the pseudo acceleration spectrum of mentioned scaled ground motions along with mean spectrum is presented. In this figure the characteristics of near-field records, especially in long periods, can be seen. Also, to consider the effect of higher modes, the building displacement was obtained from the nonlinear time history analysis.

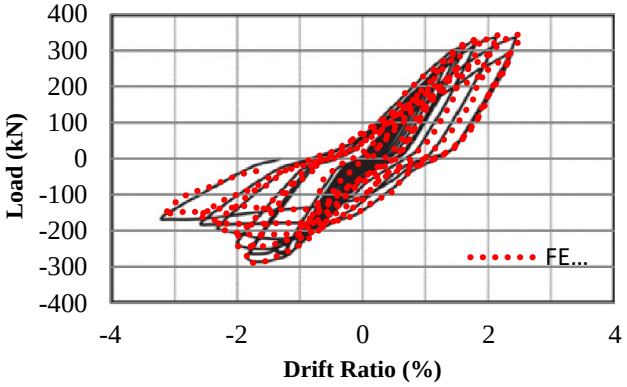

Fig. 6: Results from finite element verification

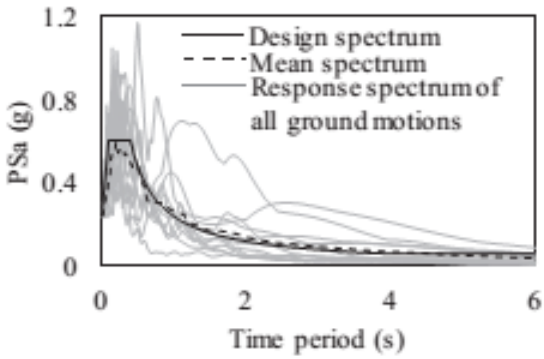

Fig.7: Pseudo acceleration spectrum of scaled ground motions along with design spectrum and mean spectrum[17]

Table 2: Near-field and Far-field seismic records used in nonlinear analysis [17]

S1.No	Event	Station	Fault distance (km)	Comp.	Mw	PGA (m/s2)	PGV (m/s)	PGV/ PGA (s)
NF1	Imperial Valley	James Rd., El Centro #5, CA #0952	5.2	230	6.5	3.6	0.96	0.26
NF2	Loma Prieta	Gilroy #3, Gilroy sewage plant #47381	6.3	90	6.9	3.62	0.44	0.12
NF3	Landers	Lucerne	2.2	260	7.3	7.11	1.33	0.19
NF4	Northridge	Pacoina Dam (downstream)	7	175	6.7	4.08	0.44	0.11
NF5	Chi-Chi	Taichung, Taiwan #TCU076	2.7	90	7.6	3.38	0.52	0.15
NF6	Kobe	Portisland	3.3	0	6.9	3.41	0.91	0.26
FF1	Imperial Valley	Superstition mountain, CA # 0286	21.8	45	6.5	1.82	0.09	0.05
FF2	Loma Prieta	Hayward . Bart Sta.	54.1	310	6.9	1.57	0.11	0.07
FF3	Landers	Coolwater	19.7	IN	7.3	2.78	0.27	0.09
FF4	Northridge	Moor Park Fire Sta.	24.7	180	6.7	2.86	0.20	0.07
FF5	Chi-Chi	Chiayi, Taiwan # CHY086	28.4	0	7.6	2.01	0.18	0.09
FF6	Kobe	Kakogawa	22.5	0	6.9	2.36	0.21	0.09

2.3 Specifications of structures

In this study, the behavior of 4, 8, and 12 story structures has been investigated using nonlinear time history analysis. The evaluated buildings in this study, are dual moment frames steel structures located in an area with a relatively high seismic hazard. The 3D structures are modeled and designed in SAP2000 (Figure 8). The height of each story is considered 3.2 meters. The roof type is a double-sided bending slab. The structures are constructed on type II soil in accordance with the AISC 341-16 [18] and ASCE seismic design regulations. The dead and live loads on the structure are considered as the residential building and in accordance with IBC as follows:

For all floors, the weight of the interior walls and the weight of the roof, (dead load) is considered 600 kg/m^2.

A load equivalent to 700 kg/m is considered as the weight of the external walls of the building and applied only to the perimeter beams.

The live load of the roof is considered 150 kg/m^2 and the live load of the floors 200 kg/m^2.

All earthquake loading assumptions were performed in accordance with the AISC LRFD and ST37 material grade is used for design steel materials.

As mentioned previously, the initial modeling and design of the structure were carreid out using SAP2000V.16 software. A summary of the sections used for beams, columns and braces is provided in Tables 3-5.

Using the mentioned assumptions, six structures were modeled and designed using the SAP2000 program. Plate girder sections for beams and box sections for columns were used (Tables 3-5).

Table 3: Design shear and sections used for the 4-story frame

Story	Design shear (kN)	Brace (mm)	(mm) Column	(mm) Beam
4	576.2988	Box 100x50-5	Box 300x300-20	270-140-20-20
3	1123.492	Box 100x50-5	Box 350x350-20	290-140-20-20
2	1633.817	Box 150x100-5	Box 350x350-20	300-150-20-20
1	1953.983	Box 200x150-5	Box 400x400-20	320-160-20-20

Table 4: Design shear and sections used for the 8-story frame

Story	Design shear (kN)	Brace (mm)	(mm) Column	(mm) Beam
8	523.908	Box 100x50-5	Box 300x300-20	270-140-20-20
7	1021.356	Box 100x50-5	Box 350x350-20	290-140-20-20
6	1485.288	Box 150x100-5	Box 350x350-20	290-140-20-20
5	1776.348	Box 150x100-5	Box 400x400-20	300-150-20-20
4	1976.562	Box 150x100-10	Box 400x400-20	300-150-20-20
3	2291.436	Box 150x100-10	Box 450x450-20	320-160-20-20
2	2393.748	Box 200x100-10	Box 450x450-20	320-160-20-20
1	2570.148	Box 200x100-10	Box 500x550-20	340-170-20-20

Table 5: Design shear and sections used for the 12-story frame

Story	Design shear (kN)	Brace (mm)	(mm) Column	(mm) Beam
12	582.12	Box 100x50-5	Box 300x300-20	270-140-20-20
11	1134.84	Box 100x50-5	Box 350x350-20	290-140-20-20
10	1650.32	Box 150x100-5	Box 350x350-20	290-140-20-20
9	1973.72	Box 150x100-5	Box 400x400-20	300-150-20-20
8	2196.18	Box 150x100-10	Box 400x400-20	300-150-20-20
7	2546.04	Box 150x100-10	Box 450x450-20	320-160-20-20
6	2659.72	Box 200x100-10	Box 450x450-20	320-160-20-20
5	2855.72	Box 200x100-10	Box 500x550-20	340-170-20-20
4	3079.16	Box 200x150-10	Box 500x500-25	340-170-20-20
3	3176.18	Box 200x150-10	Box 500x500-25	360-180-20-20
2	3348.66	Box 250x200-10	Box 550x550-25	360-180-20-20
1	3646.58	Box 250x200-10	Box 550x550-30	380-200-20-20

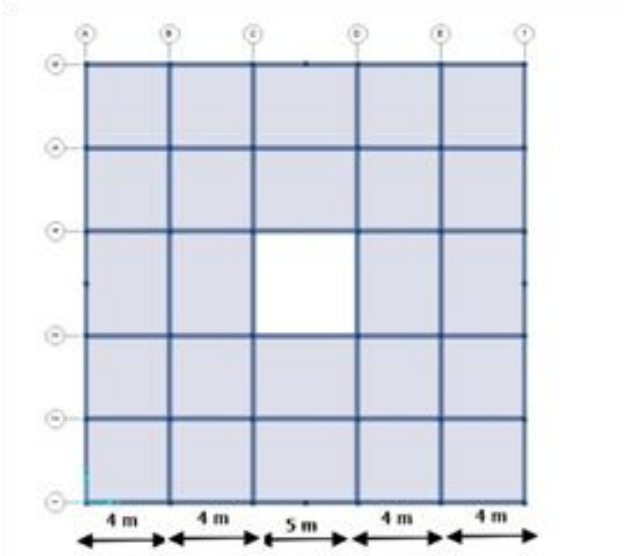

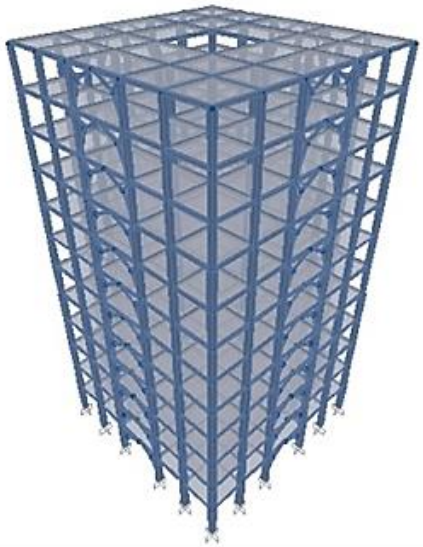

Fig. 8: 3D model of a 12-story structure modeled in SAP2000 software

3. Results and discussion

Figure 9 compares the displacements of a 4-story structure with a Y-shape brace and without a Y-shape brace under the near-field Northridge seismic record. Initially the structures remain in the elastic zone, but gradually, as the earthquake intensity increases, the structures enter a non-linear phase and the displacement of the structure increases significantly. At the beginning of the diagram in Figure 9, the amount of displacement of the structure with Y-shape brace is equal to the moment frame structure, because the earthquake has not yet reached its maximum intensity. From Figure 9 it can be pointed out that the permanent displacement of the structure with a Y-shape brace is less than the moment frame structure, therefore the Y-shape brace effectively reduces the permanent displacement in the structure.

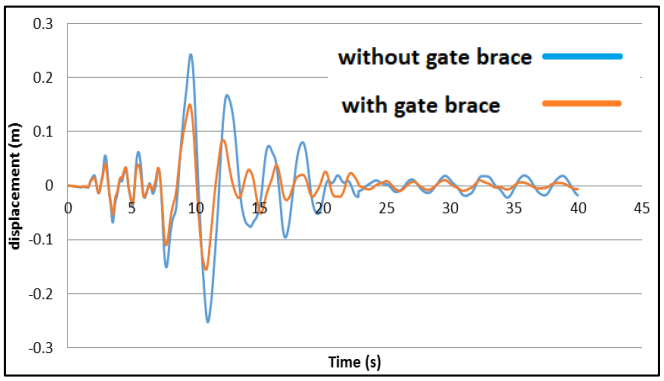

Fig. 9: Displacement of 4-story structures with Y-shape bracing and without it under the near-field Northridge earthquake (most critical case)

Also, in Figure 10, the displacement of the mass center of the roofs of structures equipped with Y-shape braces and without it under far-field earthquakes is presented. It can be clearly seen that the displacement of structures equipped with Y-shape braces is less than the structures without it. The response is compared with the same structures without Y-shape bracing.

As it can be seen in Figure 10, in general, the displacements obtained from the far-field earthquakes are less than the displacements obtained from the near-field earthquakes.

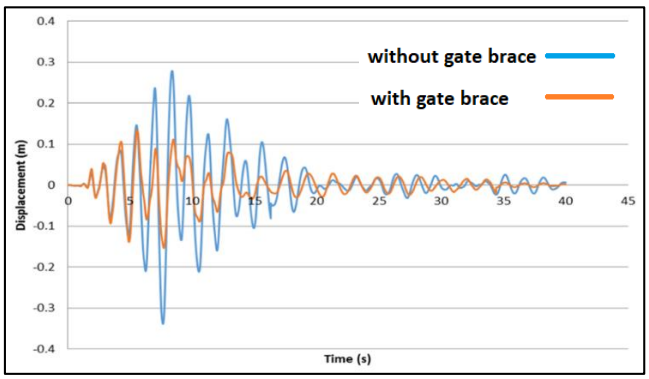

Fig. 10: Displacenment of 12-story structures with Y-shape bracing and without it under the far-field Loma Prieta earthquake (most critical case)

Figures 9 and 10 indicate that the permanent displacement of the structure with Y-shape brace is less than the moment frame structure, therefore the Y-shape brace effectively reduces the structure displacement under far-field excitations. In Figure 11, a general comparison between the responses of all the models in this research has been made. As can be seen, in the 12-story building under the Loma Prieta seismic record, the most displacement occurred under the near-field earthquake. In all the structures, the records of the near-field have caused more displacement.

The displacement of buildings under earthquakes in the far-field is smaller, this is due to the fewer number of pulses and the decreased intensity due to the distance from the fault. Also, in near-field earthquakes, a displacement pulse is created in the buildings due to the pulse-shaped movements of the earth. In the case of far-field earthquakes, due to the

more uniform distribution of energy during the duration of the earthquake, the nature of the displacement response is different. In the near-field earthquakes, for a constant PGA, the values of the relative displacement of the buildings have a positive correlation with the values of PGV and PGD of the records, but this correlation is not seen under far-field earthquakes. The progressive directivity effect, which includes a large pulse at the beginning of the ground motion velocity time history, is the most destructive phenomenon observed in strong ground motions in the near-field domain. This pulse with a large amplitude and a medium to long cycle time contains the major part of the seismic energy caused by the rupture in the fault.

3.1 Dissipated energy results

The applied input energy to an inelastic system by seismic load is dissipated by viscous damping and yielding. These energy quantities are discussed in this research. Based on the output of the energy curve caused by the Kobe earthquake on structures with and without a Y-shape brace under near-field earthquakes. The nonlinear dissipated energy in a structure equipped with Y-shape bracing is higher than the structure without it. This is due to the stable behavior of Y-shape braces. In general, it can be concluded that the structure with different heights equipped with Y-shape bracing has the ability to dissipate higher energy than the structure without Y-shape bracing. Briefly, only the obtained results under Kobe near-field earthquakes are shown because it had the most energy content between models, and energy content differences under near-field records are much more compared to far-field ones. The reason is, the earthquakes in the near-field have a very high energy content.

As shown in Figure 12 the energy content graphs, the response of structures with Y-shape braces has a much higher amount of absorbed energy, but structures without Y-shape braces show a lower value. The energy content graphs, which are related to yielding, kinematic and strain energy, are much more in structures with Y-shape braces. This is consistent with the obtained results because it can be seen further that in the system of steel moment frame without Y-shape braces, the number of plastic hinges is higher, and also the performance level in which the plastic hinges are formed is more critical.

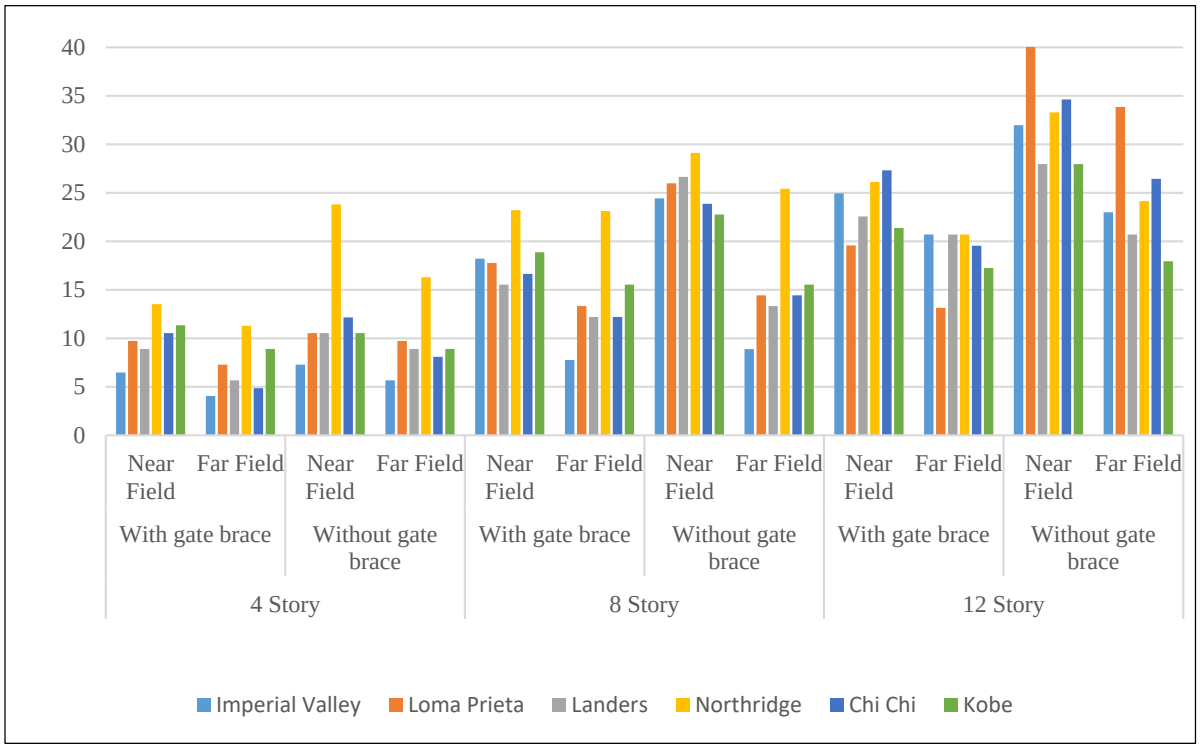

Fig. 11: Comparing roof center of mass displacement

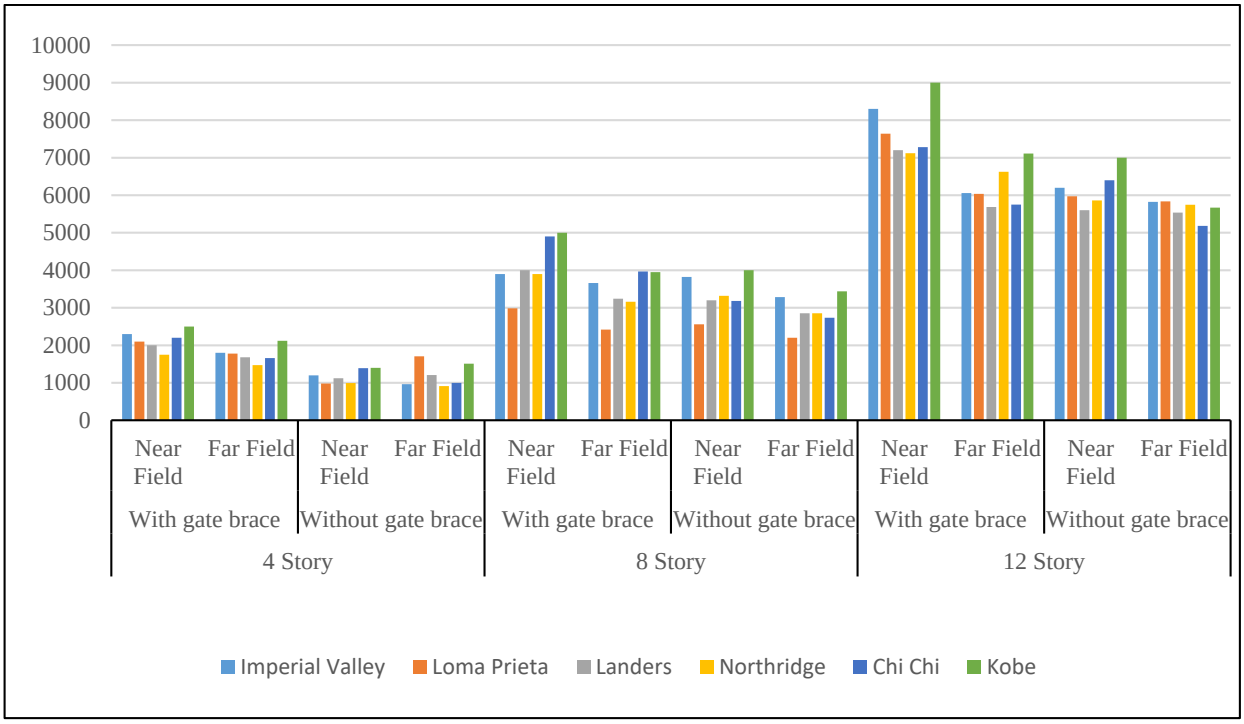

Fig. 12: Comparing dissipated energy content of different buildings

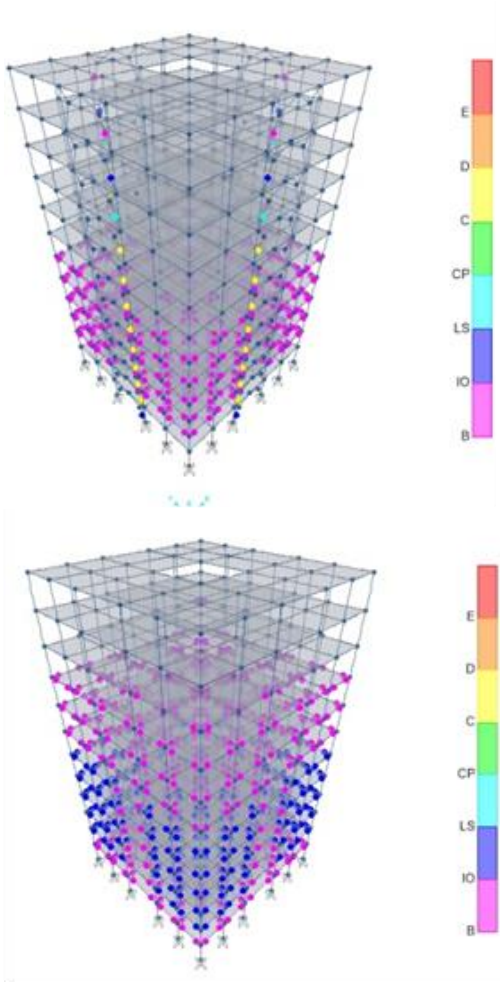

Fig. 13: Plastic hinges formed in a special moment frame structure and structure equipped with a Y-shape brace

It shows that the system equipped with a Y-shape brace is very successful in dissipating energy and the Y-shape bracing system has dissipated the seismic energy without being damaged or any failure in the members due to more damping.

Also, as shown in Figure 13, the plastic hinges formed in the beams of the special moment frame structure are much more than the plastic hinges in moment frame structures equipped with Y-shape braces. All the plastic hinges defined for the beams are of the moment type and around the strong axis of the beam (M_3). Also, the plastic hinges in the Y-shape braces are defined as axial and in the middle of the elements used in Y-shape braces. The main reason is the concentration of plastic hinges in Y-shape braces and the high seismic energy consumption in them.

4. Conclusion

To study more accurately the effects of far and near-field earthquakes on the seismic behavior of structures equipped with Y-shape bracing, the behavior of these structures was investigated, and a good match was observed between the numerical modeling results. The finite element modeling and the evaluations showed that using Y-shape braces has reduced the number and performance level of plastic hinges developed in structural beams. The use of Y-shape braces has led to an increase in the seismic energy dissipation of the structures. Due to the connection and special form of this type of braces, seismic energy depletion occurs in braces of these structures and other members of the structure remain in the elastic region. Y-shape braces had a great ability to reduce the stresses created in the studied frames especially against near-field earthquakes which have a large vertical component.

Examining the models of 4, 8, and 12-story structures with Y-shape bracing in comparison with the structure without any bracing, we see that plastic hinges are widely formed in Y-shape braces and the failure conduction is transferred to the braces which causes proper seismic behavior of the equipped structure. The seismic behavior of the structure equipped with Y-shape bracing has a significant improvement compared to the structure without bracing. Comparing the results of the energy contents showed, the near-field earthquakes has a much stronger effect than the far-field seismic response of structures equipped with Y-shape bracing. The reason for this is the high velocity and energy content of near-field earthquakes.

The use of Y-shape bracing has greatly reduced the permanent displacement in the system (in some cases up to 30%). The use of Y-shape braces causes seismic damage to be directed toward these braces and fewer plastic hinges will form in the structural beams. Y-shape braces due to the special flexible connection must be modeled with high accuracy. Therefore, the special executive details of the Y-shape braces were first modeled with precise details in Abaqus software and the software results show that the stresses are mostly focused on the element connected to the beam. Y-shape braces have a high potential in withstanding load cycles and Thid study demonstrated that buckling has occurred in the brace element connected to the beam at the end of the cycles. The results of nonlinear time history analyses shows that in Y-shape braces, the major plastic hinges are formed in the element connected to the beam or column, and the element contiguous to the beam-column and connection in the corner of the frame remains almost elastic. The results of the research shows an 18% increase in the amount of dissipated energy in the models under the near-field earthquakes, compared to the far-field earthquakes either in the presence or absence of the Y-shape brace. In far-field earthquakes, the absence of the Y-shape brace on average has reduced the amount of dissipated energy by 20.6%. In near-field earthquakes, the absence of the Y-shape brace on average has reduced the amount of dissipated energy by 29%. A 22.5% increase is observed in the amount of roof center mass displacement in the models under the near-field earthquakes, compared to the far-field earthquakes either in the presence or absence of the Y-shape brace. In far-field earthquakes, the absence of the Y-shape brace on average has increased the amount of dissipated energy by 39%. In near-field earthquakes, the absence of the Y-shape brace on average has increased the amount of dissipated energy by 44.3%.

Near-field earthquakes have a more significant impact on energy dissipation and structural response than far-field earthquakes due to their high velocity and energy. Also, finite element modeling confirms that Y-shape bracing reduces both the number and severity of plastic hinges in beams and increases overall seismic energy dissipation using bracing. The special geometry and connections of the Y-shape braces enable them to absorb seismic energy efficiently, protecting the main structural frame. This effect is especially pronounced under near-field earthquakes, which have large vertical components and high energy content.

References

[1] F. Farheen and S. P. Akshara, “Comparison of Seismic Performance of Knee Braces in Steel Frames with Y Shaped Eccentric Braces,” in *National Conference on Structural Engineering and Construction Management*, 2019, pp. 551–562.

[2] E. P. Popov, K. Kasai, and M. D. Engelhardt, “Advances in design of eccentrically braced frames,” *Earthquake Spectra*, vol. 3, no. 1, pp. 43–55, 1987.

[3] S. Najafi, K. Saboohian, and S. Borzoo, “The Effect of Y-Shaped Brace Configuration on Its Seismic Behavior,” *International Journal of Steel Structures*, pp. 1–19, 2022.

[4] P. Heinemann and D.-N. Isopescu, “Experimental and Numerical Case Studies about Two-Dimensional CHS Joints with a Symmetrical Y-Shape,” *Materials*, vol. 15, no. 9, p. 3179, 2022.

[5] S. M. Zamani, A. Vafaei, A. A. Aghakouchak, and C. Desai, “Experimental investigation of steel frames braced with symmetrical pairs of y-shaped concentric bracings,” *International Journal of Steel Structures*, vol. 11, no. 2, pp. 117–131, 2011.

[6] M. R. S. Nezhad and M. M. Sahebi, “A numerical and experimental seismic study on the ductile tubular elements and their performance in Y-Shaped braces,” in *Structures*, Elsevier, 2022, pp. 737–749.

[7] M. Ghiasvandand, M. Alirezaei, S. M. Mirhosseini, and E. Zeighami, “Experimental and parametric study of a novel braced system to improve seismic performance,” in *Structures*, Elsevier, 2022, pp. 229–242.

[8] A. Shahiditabar, H. Moharrami, and H. H. Snijder, “Quantification of seismic performance factors of self-centered y-shaped braced frames,” *J Constr Steel Res*, vol. 194, p. 107304, 2022.

[9] F. M. Mazzolani, G. Della Corte, and G. Cantisani, “Seismic Upgrading of an Existing Steel Structure Using Inverted Y-braces,” in *International Conference on the Behaviour of Steel Structures in Seismic Areas*, Springer, 2022, pp. 890–897.

[10] T. Li, M. Su, Y. Sui, and L. Ma, “Real-time hybrid simulation on high strength steel frame with Y-shaped eccentric braces,” *Eng Struct*, vol. 226, p. 111369, 2021.

[11] Y. Minaei, M. Mashayekhi, and M. Sarcheshmehpour, “Incremental Dynamic Analysis of Mid-Rise Buildings with Buckling Restrained Brace Frame System under Pulse-Like Near-Fault Ground Motions,” *Journal of Rehabilitation in Civil Engineering*, pp. 47–67, 2025.

[12] A. Majdi, M. Mashayekhi, and A. Sadeghi-Movahhed, “Effect of near-fault earthquake characteristics on seismic response of mid-rise structures with triple friction pendulum isolator,” *Journal of Rehabilitation in Civil Engineering*, vol. 12, no. 1, pp. 47–62, 2024.

[13] H. A. Moghaddam and H. Estekanchi, "On the characteristics of an off-centre bracing system," *J Constr Steel Res*, vol. 35, no. 3, pp. 361–376, 1995.

[14] S. M. Zamani, A. Vafaei, C. Desai, and M. Rasouli, "Experimental investigation of behavior of steel frames with y-shaped concentric bracing," *J Constr Steel Res*, vol. 70, pp. 12–27, 2012.

[15] British Standard EN10025-2, "Hot rolled products of structural steels—," 2004.

[16] M. Bahirai, M. Gerami, and V. Bahaari Zargar, "Postannealing mechanical properties of structural steel St37," *Journal of Materials in Civil Engineering*, vol. 32, no. 7, p. 04020152, 2020.

[17] S. Gorai and D. Maity, "Seismic response of concrete gravity dams under near field and far field ground motions," *Eng Struct*, vol. 196, p. 109292, 2019.

[18] AISC, *Seismic provisions for structural steel buildings*, no. 2. American Institute of Steel Construction, 2016.